Effects of Surface Area, Free Volume, and Heat of Adsorption on Hydrogen Uptake in Metal−Organic Frameworks

Houston Frost,[†] Tina Düren,[‡] and Randall Q. Snurr*,[†]

Department of Chemical and Biological Engineering, Northwestern University, 2145 Sheridan Road, Evanston, Illinois, 60208, and Institute for Materials and Processes, School of Engineering and Electronics, University of Edinburgh, King's Buildings, Edinburgh EH9 3JL, United Kingdom

Received: January 20, 2006; In Final Form: March 21, 2006

Grand canonical Monte Carlo simulations were performed to predict adsorption isotherms for hydrogen in a series of 10 isoreticular metal−organic frameworks (IRMOFs). The results show acceptable agreement with the limited experimental results from the literature. The effects of surface area, free volume, and heat of adsorption on hydrogen uptake were investigated by performing simulations over a wide range of pressures on this set of materials, which all have the same framework topology and surface chemistry but varying pore sizes. The results reveal the existence of three adsorption regimes: at low pressure (loading), hydrogen uptake correlates with the heat of adsorption; at intermediate pressure, uptake correlates with the surface area; and at the highest pressures, uptake correlates with the free volume. The accessible surface area and free volume, calculated from the crystal structures, were also used to estimate the potential of these materials to meet gravimetric and volumetric targets for hydrogen storage in IRMOFs.

Introduction

Metal−organic frameworks are a new class of microporous materials with potential applications in adsorption separations, catalysis, and gas storage.[1−4] They are synthesized in a building block approach from metal or metal oxide vertexes interconnected by organic linkers. An example of one class of MOFs is shown in Figure 1. The materials illustrated in Figure 1 were discovered by Yaghi and co-workers and are known as isoreticular metal−organic frameworks or IRMOFs.[5−7] They feature oxide-centered Zn_4O tetrahedra each connected by six dicarboxylate linkers, resulting in extended 3-dimensional cubic networks having very high porosity. A variety of linker molecules can be used to create an entire family of materials having different pore sizes and containing different chemical functionalities within the linkers but all with the same basic framework topology. In addition, different metal corners and different linkage chemistries can yield a wide variety of other framework topologies.[1,8−11]

The building-block approach has generated much excitement about the possibility to design new nanoporous materials. For example, within the IRMOF family, if one conceives of a new linker molecule, say with a desired chemical functionality, there is a good chance that it can be incorporated into an IRMOF if the required carboxylate groups can be synthesized at the ends and if the linker is fairly rigid.[12,13] However, if MOFs are to be truly designed for particular applications, we need a better understanding of how the key structural features affect adsorption of guest molecules. This paper will focus on gas storage applications, where the adsorption isotherm is of particular importance, but the same considerations are clearly applicable to adsorption separations with MOFs.

Alternative fuels such as hydrogen and natural gas have been studied extensively for their potential use in next-generation vehicles. A key issue in implementing alternative fuels in vehicles is how to store the fuel safely and cost efficiently, which requires a way to keep the fuel at high densities at reasonable pressures. MOFs have been investigated for use in this application for their ability to adsorb both methane,[7,14,15] the primary component of natural gas, and hydrogen.[5,8,16−19]

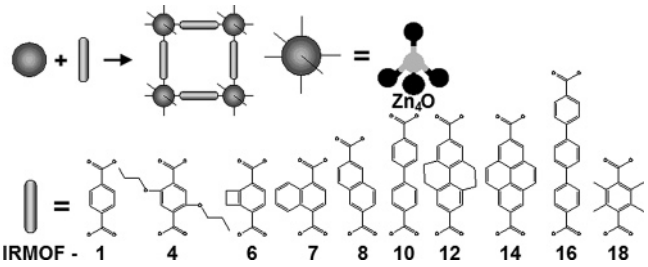

Figure 1. The geometry and building blocks of IRMOF materials studied in this work.

To maximize gas storage by physisorption, much attention has focused on the role of surface area.[8,14,18,20−24] Some of the MOFs synthesized to date have incredibly high surface areas. For example MOF-177 has a surface area of 4500 $m^2\ g^{-1}$ estimated from nitrogen adsorption.[20] This is much higher than the zeolite with the highest surface area, namely zeolite Y at 904 $m^2\ g^{-1}$, and even higher than activated carbons, which have surface areas around 2000 $m^2\ g^{-1}$.[20] Adsorption is primarily due to interactions of guest molecules with atoms of the adsorbent walls, so it seems logical that a high surface area—either per unit mass or per unit volume—should be desirable for high uptake. Düren et al.[14] examined a variety of microporous materials, including MOFs, zeolites, and carbon nanotubes, using atomistic grand canonical Monte Carlo (GCMC) simulations and found that adsorption of methane at 35 bar and 298 K does correlate with the surface area. They found, however, that the free volume and the strength of adsorbent/guest interactions also play a role and that these factors are interlinked in a nontrivial way.

* Address correspondence to this author. E-mail: snurr@northwestern.edu.
[†] Northwestern University.
[‡] University of Edinburgh.

10.1021/jp060433+ CCC: $33.50
Published on Web 04/22/2006

The development of simple heuristics to avoid the need for full GCMC simulations or adsorption experiments would be helpful to researchers synthesizing new materials. In this paper, we revisit the role of surface area, free volume, and adsorbent/guest energetics in determining adsorption of small molecules in microporous materials. In contrast to the work of Düren et al.,[14] we consider a series of materials all having the same framework topology and the same "wall" chemistry. We used GCMC simulations to predict adsorption of hydrogen and methane in the ten IRMOFs shown in Figure 1. In addition, rather than focusing just on the adsorption at a single pressure, we considered the full range of loadings from very dilute to complete pore filling.

Simulation Methods

Hydrogen adsorption in the IRMOFs was simulated with GCMC[25,26] by using our multipurpose simulation code Music.[27] Gas-phase fugacities for hydrogen were calculated with the Peng−Robinson equation of state. A united-atom model was used for the guest molecules, and an atomistic model was used for the porous frameworks, which were considered rigid with atoms at the positions reported from crystallography.[5−7] All interatomic interactions were modeled with a standard Lennard-Jones potential. The Lennard-Jones parameters for the hydrogen molecule are known from experimental work[28] and have been used in similar simulation studies by Dakrim,[29] whereas the parameters for the framework atoms were taken from the DREIDING force field.[30] Lorentz−Berthelot mixing rules were employed to calculate sorbate/framework parameters. Interactions beyond 12.8 Å were neglected. The Lennard-Jones parameters can be found in Table S1 in the Supporting Information. For each point on the isotherm, one million Monte Carlo steps were performed. A Monte Carlo step consisted of one of the following: insertion of a new molecule, deletion of an existing molecule, or translation of an existing molecule. Rotation and intramolecular moves were unnecessary as the H_2 molecule was represented as a single sphere (united atom model). The first 600 000 steps were used for equilibration, and the last 400 000 steps were used to calculate the ensemble averages. Adsorption isotherms were calculated for hydrogen in the ten IRMOFs shown in Figure 1 at 77 K and pressures up to 120 bar.

Molecular simulation predicts the absolute number of sorbate molecules within the framework material at the given gas-phase conditions, whereas experimental measurements yield the excess amount adsorbed. The excess adsorption is the amount of sorbate within the adsorbent above and beyond what is found in the ambient gas phase. The conversion from absolute to excess sorption can be performed as follows:

$$N_{ex} = N_{abs} - V_g \rho_g \quad (1)$$

The excess adsorption, N_{ex}, is determined from the absolute adsorption, N_{abs}, by subtracting the pore volume of the adsorbent, V_g, calculated as described by Myers and Monson,[31] multiplied by the density of the ambient gas phase, ρ_g, calculated with the Peng−Robinson equation of state.

The available surface area and free volume were calculated for all IRMOFs by using a numerical Monte Carlo integration technique. The surface area was calculated by "rolling" a probe molecule with a diameter equal to the Lennard-Jones σ parameter for H_2 ($\sigma = 2.958$ Å) over the framework surface. Surface area is highly dependent on the probe size used for measurement, and calculating the surface area in this manner provides the amount of area accessible to hydrogen molecules. The probe was randomly inserted around the surface of each framework atom in turn, which were also given sizes equal to their Lennard-Jones σ parameters, and tested for overlap. The fraction of probes that did not overlap with other framework atoms was used to calculate the available surface area. The free volume (different than V_g above) was calculated by using a similar method of trial insertions within the entire volume of the unit cell. A probe size of 0 Å was used to enable us to determine the total free volume in the unit cell. Probing the material in this manner enables us to determine the volume of the simulation cell that is not occupied by framework atoms. This method of calculating free volume is based solely on the system geometry, whereas the pore volume, V_g, is based on a thermodynamic definition. The isosteric heat of adsorption, Q_{st}, was calculated at low loadings, between 0 and 0.5 bar, as described by Snurr et al.[32] The isosteric heat was found to be approximately constant within this pressure range.

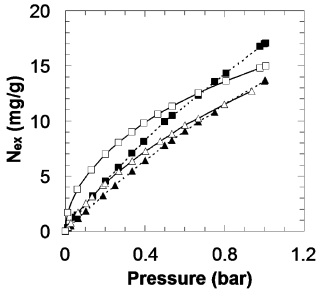

Figure 2. Simulated and experimental adsorption isotherms for IRMOF-1 and IRMOF-8 at 77 K: ▲, IRMOF-1 simulation; △, IRMOF-1 experiment; ■, IRMOF-8 simulation; □, IRMOF-8 experiment. The lines were added to guide the eye.

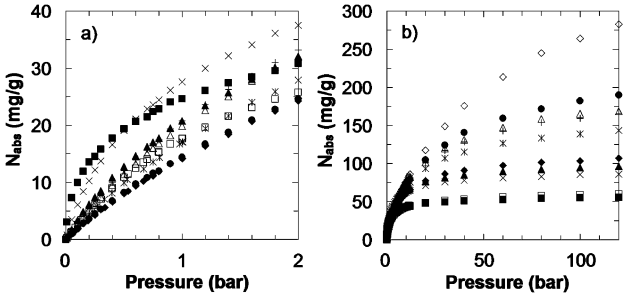

Figure 3. (a) Low-pressure simulation adsorption isotherms at 77 K and (b) High-pressure simulation adsorption isotherms at 77 K: ◆, IRMOF-1; ■, IRMOF-4; ▲, IRMOF-6; ×, IRMOF-7; ∗, IRMOF-8; ●, IRMOF-10; +, IRMOF-12; △, IRMOF-14; ◇, IRMOF-16; □, IRMOF-18.

Results and Discussion

Simulations of hydrogen adsorption were performed at 77 K to compare against experimental data from the literature. As Figure 2 shows, the simulation results are in reasonable agreement with the experimental data of Rowsell et al.[5] for IRMOF-1 and -8, but the concavity of the adsorption isotherms deviates somewhat. Agreement for IRMOF-18 (not shown) is not as good, as simulation overestimates adsorption by about a factor of 2 throughout the pressure range. Several other research groups have reported similar results recently with somewhat different force fields.[33−35] Yang and Zhong[34] obtained better results for these three MOFs by fitting the force field parameters. Garberoglio[35] discuss the effects of changing the force field, for example, by adding a Coulomb potential. We did not attempt to improve the force field, but the results are reasonably good given the simplicity of the model.[36]

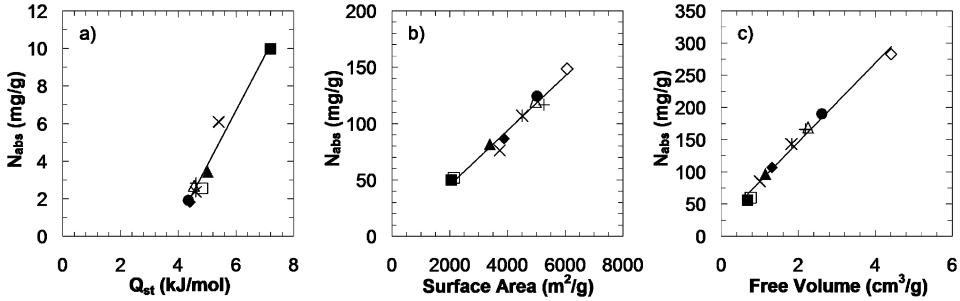

Figure 4. (a) Amount adsorbed at 0.1 bar vs isosteric heat of adsorption. (b) Amount adsorbed at 30 bar vs accessible surface area. (c) Amount adsorbed at 120 bar vs free volume. The symbols are the same as in Figure 3.

Most of the materials are predicted to have very similar heats of adsorption at low loadings, between 4.5 and 5.5 kJ/mol. These values agree well with numbers reported in the literature from experiment[37,39] and quantum chemical calculations.[16,33,40,41] IRMOF-4 has a noticeably higher heat of adsorption at low loading than the other materials (7.2 kJ/mol) due to the small pore size and the high number of framework atoms resulting from the alkyl chains.

Absolute adsorption isotherms for the ten IRMOFs considered are presented in Figure 3 in terms of gravimetric uptake. At low pressures (Figure 3a), IRMOFs-4 and -7 show the highest uptake of hydrogen, but at pressures above about 15 bar (Figure 3b), IRMOF-16 displays the largest uptake per gram of sorbent. The qualitative reason for this crossing of the isotherms is well understood from the adsorption literature.[42,43] At low loadings, materials with the strongest enthalpic interactions with sorbed molecules show the highest levels of adsorption. These tend to be materials with narrow pores, such as IRMOFs-1, -4, -6, and -7, because small pores increase the interaction between hydrogen and the framework.[44,45] However, materials with narrow pores also have the highest framework densities (see Table S2 in the Supporting Information) and thus the lowest amounts of free void space per gram of material. Therefore, at the highest pressures when the pores are nearly filled, the materials with the largest free volumes have more room for guest molecules and consequently show the highest uptake.

To make this idea more quantitative, we plotted the amount adsorbed at low pressure (0.1 bar) against the isosteric heat of adsorption and the amount adsorbed at high pressure (120 bar) against the free volume of the frameworks. The results, presented in Figure 4a,c, show that there are excellent correlations in both cases. Between these two limiting cases, one might expect that the surface area would be important. In Figure 4b, the amount of hydrogen adsorbed at an intermediate pressure (30 bar) is plotted as a function of the surface area per gram. An excellent correlation is also found in this case.

It appears that three different adsorption regimes can be identified. At low pressure, the amount adsorbed correlates with the heat of adsorption. At intermediate pressures, the amount adsorbed correlates with the surface area. And at the highest pressures, the amount adsorbed correlates with the free volume. Figure 4 shows these correlations using a gravimetric basis, but the correlations hold on a volumetric basis as well. This simply requires dividing the specific surface area, the specific free volume, and the amount adsorbed per gram by the framework density. Furthermore, the correlations also hold for the excess amount adsorbed, although the correlations are slightly weaker. Absolute adsorption was used here because it is more closely tied to the physics underlying the correlations.

As a further demonstration that these three regimes hold, we tested for correlation of the amount adsorbed at each of the three

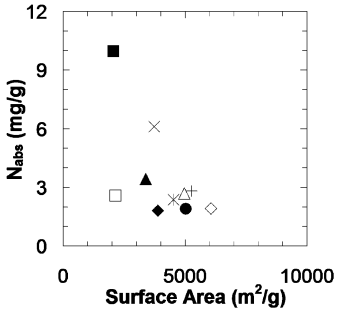

Figure 5. Amount adsorbed at 0.1 bar vs accessible surface area. There is no correlation. The symbols are the same as in Figure 3.

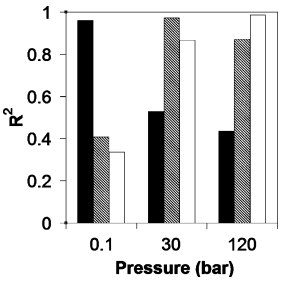

Figure 6. Coefficient of multiple determination (R^2) for correlation of amount adsorbed with: solid bar, heat of adsorption; hatched bar, surface area; and open bar, free volume.

pressures with all three properties (heat of adsorption, surface area, and free volume). For example, in Figure 5, the amount adsorbed at 0.1 bar is plotted against the surface area, and it can be seen that there is no correlation. Similarly there is no correlation of the amount adsorbed at 0.1 bar with the free volume. A summary of these determinations is given in Figure 6, which shows the coefficient of multiple determination (R^2) for each of the nine cases. R^2 represents the fraction of variability in the observations accounted for by the first-order linear regression equation used, that is, the fraction of the total variability in the data that is captured by the regression equation, the remainder of which is considered random noise. The R^2 values for adsorption vs heat of adsorption in Figure 6 clearly indicate a linear regression is not adequate to quantify adsorption at 30 and 120 bar. Similarly R^2 values for adsorption vs surface area indicate a linear regression is best at intermediate pressures. Finally, the R^2 values for adsorption vs free volume show that as pressure increases the quality of regression improves. There exists a loose correlation between surface area and free volume for this series of materials ($R^2 = 0.87$), and this is the cause of the high R^2 values for the surface area correlation at 120 bar and the free volume correlation at 30 bar. The correlations in Figure 4 all pass a significance of regression test[46] with 99.99% confidence or greater, and the residuals have been found to be

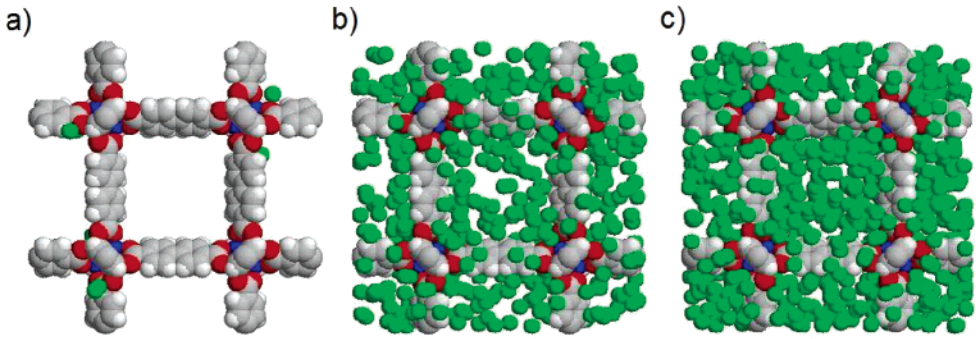

Figure 7. Snapshots of hydrogen adsorption in IRMOF-10: (a) 0.1, (b) 30, and (c) 120 bar.

TABLE 1: Potential Gravimetric Hydrogen Uptake Based on Accessible Surface Area and Free Volume[52]

material	accessible surface area for H_2 (m^2/g)	free vol (cm^3/g)	H_2 uptake (wt %) assuming $\phi = 0.55$[a]	H_2 uptake (wt %) assuming $\phi = 0.91$[a]	H_2 uptake (wt %) assuming liquid H_2 within free volume	H_2 uptake (wt %) assuming solid H_2 within free volume
IRMOF-1	3882	1.315	10.4	17.2	9.3	11.6
IRMOF-4	2056	0.694	5.5	9.1	4.9	6.1
IRMOF-6	3395	1.142	9.1	15.0	8.1	10.0
IRMOF-7	3730	1.013	10.0	16.5	7.2	8.9
IRMOF-8	4518	1.834	12.1	20.0	13.0	16.1
IRMOF-10	5029	2.615	13.5	22.3	18.6	23.0
IRMOF-12	5267	2.188	14.1	23.3	15.5	19.3
IRMOF-14	4964	2.259	13.3	22.0	16.0	19.9
IRMOF-15	6075	1.962	16.3	26.9	13.9	17.3
IRMOF-16	6055	4.413	16.2	26.8	31.3	38.8
IRMOF-18	2148	0.780	5.8	9.5	5.5	6.9

[a] ϕ is the coverage fraction; the liquid H_2 density at 20.3 K and 1 atm is 70.96 g/L; the solid H_2 density at 13.8K and 1 atm is 88 g/L.[53,54]

TABLE 2: Potential Volumetric Hydrogen Uptake Based on Accessible Surface Area and Free Volume[52]

material	accessible surface area for H_2 (m^2/cm^3)	void fraction	H_2 uptake (g/L) assuming $\phi = 0.55$	H_2 uptake (g/L) assuming $\phi = 0.91$	H_2 uptake (g/L) assuming liquid H_2 within free volume	H_2 uptake (g/L) assuming solid H_2 within free volume
IRMOF-1	2290	0.780	61.4	101.5	55.3	68.6
IRMOF-4	1770	0.597	47.4	78.5	42.4	52.6
IRMOF-6	2207	0.745	59.1	97.8	52.9	65.6
IRMOF-7	2648	0.718	71.0	117.4	51.0	63.2
IRMOF-8	2024	0.822	54.2	89.7	58.3	72.3
IRMOF-10	1660	0.860	44.5	73.6	61.0	75.7
IRMOF-12	2001	0.832	53.6	88.7	59.1	73.2
IRMOF-14	1837	0.843	49.2	81.4	59.8	74.2
IRMOF-15	2509	0.808	67.2	111.2	57.3	71.1
IRMOF-16	1241	0.905	33.3	55.0	64.2	79.6
IRMOF-18	1837	0.667	49.2	81.4	47.3	58.7

normally distributed uncorrelated random variables with a mean of zero and constant variance.

Visualizations of molecular siting within IRMOF-10 are shown in Figure 7 in the three different pressure/loading regimes. Figure 7a shows that at low pressure hydrogen molecules are mostly near the zinc corners, which are the most favorable energetic adsorption regions due to the high concentration of framework atoms. This has also been reported by other simulation studies,[33,34,47] and inelastic neutron scattering experiments have also found that hydrogen tends to adsorb near the zinc corners.[48] Figure 7b shows that at 30 bar, molecules adsorb preferentially in the corners and along the linker molecules, with fewer molecules in the centers of the cavities. Figure 7c displays the limiting adsorption behavior where hydrogen fills the majority of the void regions of the material.

The three adsorption regimes were also found for methane in IRMOFs at 298 K with pressures of 0.1, 50, and 200 bar.[49] Presumably the existence of these three regimes is a general result that holds for other adsorbates and adsorbents because the fundamental physics of adsorption thermodynamics is the same. It should be noted that the transitions between regimes do not occur at distinct pressures; rather they occur gradually as pressure, and hence the loading in the pores, is increased. In addition, the specific pressures corresponding to low, intermediate, and high pressures will be different for different systems and also for different temperatures. This is because the correlations are a result of the extent of loading rather than tied directly to any pressure values.

The discovery of the excellent correlations in Figure 4 was mainly made possible by the recent synthesis of these materials that all have the same framework topology, constituent atom types, and wall chemistry. When Düren et al.[14] performed a similar analysis for methane adsorption in IRMOFs, carbon nanotubes, and zeolites, they found a correlation of the amount adsorbed at 35 bar with the surface area, but the correlation was a band of data points rather than the single line seen in Figure 4b.

The calculated surface areas and free volumes allow for a simple estimate of an upper bound on the adsorption capacity, and we used this to examine the potential of these 10 IRMOFs to meet the targets for hydrogen storage set by the U.S. Department of Energy.[50] The 2010 targets are 6 wt % and 45

g/L, and the 2015 targets are 9 wt % and 81 g/L. First, we considered the surface area. In a simple "back-of-the-envelope" calculation, we took the accessible surface area of each material and asked what loading would be possible if monolayer adsorption could be achieved. Two different packing models of molecules were explored: a randomly packed monolayer[51] with a coverage fraction of 0.55 and a hexagonally packed monolayer with a coverage fraction of 0.91. Hydrogen molecules were assumed to be spherical with a diameter of 2.958 Å. The accessible surface area per gram of sorbent was multiplied by the coverage fraction and then divided by the cross-sectional area of a hydrogen molecule to estimate the potential gravimetric hydrogen uptake, naively assuming monolayer adsorption. The results, presented in columns 4 and 5 of Table 1, indicate that the upper bounds for hydrogen uptake in these IRMOF materials are above the DOE gravimetric targets of 6 or 9 wt %. In a similar simple calculation, we took the free volume per gram for each material and calculated the gravimetric uptake of hydrogen if the void space could be filled with hydrogen at either its liquid or solid density. These results, shown in columns 6 and 7 of Table 1, are also encouraging.

Table 2 shows analogous results on a volumetric basis. The results are mostly above the DOE 2010 volumetric target of 45 g/L, but the 2015 target (81 g/L) may be difficult to meet. This is, perhaps, not surprising, given that solid hydrogen (at 13.8 K and 1 atm) has a density of 88 g/L, which is only slightly higher than the 2015 target.

It should be kept in mind that the results in Tables 1 and 2 do not come from GCMC simulations, but only from the accessible surface area and free volume calculated from the crystal structures, along with an assumed monolayer coverage or an assumed density in the pores. The results in Tables 1 and 2 do not indicate what pressures would be required to achieve these loadings at room temperature. The assumption of uniform monolayer coverage or uniform filling of the void space is an upper limit on adsorption, so these simple calculations are a potentially valuable screening tool that could be applied to new materials very quickly.

Conclusions

Molecular simulations of hydrogen adsorption isotherms in IRMOF materials revealed the existence of three distinct regimes. Comparing different materials, the amount adsorbed can be correlated with the heat of adsorption at low pressures (loadings), the surface area at intermediate pressures, and the free volume at high pressures. Because the materials studied all have the same framework topology and surface chemistry, the transitions between the regimes occurred at similar pressures and this provided for the excellent correlations. For materials of differing topologies and surface chemistry, the correlations will not be as good,[14] but the surface area and free volume are still clearly important characteristics in evaluating any potential hydrogen storage adsorbent.

Using the surface areas and free volumes calculated from the crystal structures, we made simple estimates of the potential of selected IRMOFs for hydrogen storage by assuming either monolayer coverage on the entire surface area or complete filling of the free volume with the density of liquid or solid hydrogen. The results indicate that IRMOFs are promising materials for meeting established hydrogen storage targets due to their very high surface areas and free volumes. A remaining challenge is to design new materials with increased heats of adsorption so that the desired densities of hydrogen can be concentrated within these materials at reasonable temperatures and pressures.

Acknowledgment. This work was supported by the Department of Energy (DEFG02-1ER15244). The authors thank Profs. Joseph Hupp and Omar Yaghi for helpful discussions.

Supporting Information Available: Lennard-Jones parameters and properties of the IRMOF materials. This material is available free of charge via the Internet at http://pubs.acs.org.

References and Notes

(1) Janiak, C. *Dalton Trans.* **2003**, 2781.
(2) Kitagawa, S.; Kitaura, R.; Noro, S. *Angew. Chem., Int. Ed.* **2004**, *43*, 2334.
(3) James, S. L. *Chem. Soc. Rev.* **2003**, *32*, 276.
(4) Snurr, R. Q.; Hupp, J. T.; Nguyen, S. T. *AIChE J.* **2004**, *50*, 1090.
(5) Rowsell, J. L. C.; Millward, A. R.; Park, K. S.; Yaghi, O. M. *J. Am. Chem. Soc.* **2004**, *126*, 5666.
(6) Li, H.; Eddaoudi, M.; O'Keeffe, M.; Yaghi, O. M. *Nature* **1999**, *402*, 276.
(7) Eddaoudi, M.; Kim, J.; Rosi, N.; Vodak, D.; Wachter, J.; O'Keefe, M.; Yaghi, O. M. *Science* **2002**, *295*, 469.
(8) Kesanli, B.; Cui, Y.; Smith, M. R.; Bittner, E. W.; Bockrath, B. C.; Lin, W. B. *Angew. Chem., Int. Ed.* **2005**, *44*, 72.
(9) Ma, B. Q.; Mulfort, K. L.; Hupp, J. T. *Inorg. Chem.* **2005**, *44*, 4912.
(10) Erxleben, A. *Coord. Chem. Rev.* **2003**, *246*, 203.
(11) Rosseinsky, M. J. *Microporous Mesoporous Mater.* **2004**, *73*, 15.
(12) Yaghi, O. M.; O'Keeffe, M.; Ockwig, N. W.; Chae, H. K.; Eddaoudi, M.; Kim, J. *Nature* **2003**, *423*, 705.
(13) Rowsell, J. L. C.; Yaghi, O. M. *Microporous Mesoporous Mater.* **2004**, *73*, 3.
(14) Düren, T.; Sarkisov, L.; Yaghi, O. M.; Snurr, R. Q. *Langmuir* **2004**, *20*, 2683.
(15) Seki, K. *Chem. Commun.* **2001**, 1496.
(16) Rowsell, J. L. C.; Yaghi, O. M. *Angew. Chem., Int. Ed.* **2005**, *44*, 4670.
(17) Pan, L.; Sander, M. B.; Huang, X. Y.; Li, J.; Smith, M.; Bittner, E.; Bockrath, B.; Johnson, J. K. *J. Am. Chem. Soc.* **2004**, *126*, 1308.
(18) Chun, H.; Dybtsev, D. N.; Kim, H.; Kim, K. *Chem. Eur. J.* **2005**, *11*, 3521.
(19) Ferey, G.; Latroche, M.; Serre, C.; Millange, F.; Loiseau, T.; Percheron-Guegan, A. *Chem. Commun.* **2003**, 2976.
(20) Chae, H. K.; Siberio-Perez, D. Y.; Kim, J.; Go, Y.; Eddaoudi, M.; Matzger, A. J.; O'Keeffe, M.; Yaghi, O. M. *Nature* **2004**, *427*, 523.
(21) Langmi, H. W.; Walton, A.; Al-Mamouri, M. M.; Johnson, S. R.; Book, D.; Speight, J. D.; Edwards, P. P.; Gameson, I.; Anderson, P. A.; Harris, I. R. *J. Alloys Compd.* **2003**, *356*, 710.
(22) Menon, V. C.; Komarneni, S. *J. Porous Mater.* **1998**, *5*, 43.
(23) Nijkamp, M. G.; Raaymakers, J.; van Dillen, A. J.; de Jong, K. P. *Appl. Phys. A: Mater. Sci. Process.* **2001**, *72*, 619.
(24) Texier-Mandoki, N.; Dentzer, J.; Piquero, T.; Saadallah, S.; David, P.; Vix-Guterl, C. *Carbon* **2004**, *42*, 2744.
(25) Allen, M. P.; Tildesley, D. J. *Computer Simulations of Liquids*; Clarendon Press: Oxford, UK, 1987.
(26) Frenkel, D.; Smit, B. *Understanding of Molecular Simulations*: *from Algorithms to Applications*, 2nd ed.; Academic Press: San Diego, CA, 2002.
(27) Gupta, A.; Chempath, S.; Sanborn, M. J.; Clark, L. A.; Snurr, R. Q. *Mol. Simul.* **2003**, *29*, 29.
(28) Michels, A.; Degraaff, W.; Tenseldam, C. A. *Physica* **1960**, *26*, 393.
(29) Darkrim, F.; Aoufi, A.; Malbrunot, P.; Levesque, D. *J. Chem. Phys.* **2000**, *112*, 5991.
(30) Mayo, S. L.; Olafson, B. D.; Goddard, W. A. *J. Phys. Chem.* **1990**, *94*, 8897.
(31) Myers, A. L.; Monson, P. A. *Langmuir* **2002**, *18*, 10261.
(32) Snurr, R. Q.; Bell, A. T.; Theodorou, D. N. *J. Phys. Chem.* **1993**, *97*, 13742.
(33) Sagara, T.; Klassen, J.; Ganz, E. *J. Chem. Phys.* **2004**, *121*, 12543.
(34) Yang, Q. Y.; Zhong, C. L. *J. Phys. Chem. B* **2005**, *109*, 11862.
(35) Garberoglio, G.; Skoulidas, A. I.; Johnson, J. K. *J. Phys. Chem. B* **2005**, *109*, 13094.
(36) After completion of this work, three experimental papers appeared reporting adsorption isotherms for hydrogen in IRMOFs at 77 K and pressures up to 80 bar.[37−39] Simulations and experiments show similar values for the saturation pressures, but there is some discrepancy in the loading (also among the experimental reports). Further work is needed to uncover the reasons for these discrepancies, but the conclusions of this paper should not be affected.
(37) Dailly, A.; Vajo, J. J.; Ahn, C. C. *J. Phys. Chem. B* **2006**, *110*, 1099.

(38) Wong-Foy, A. G.; Matzger, A. J.; Yaghi, O. M. *J. Am. Chem. Soc.* **2006**, *128*, 3494.

(39) Panella, B.; Hirscher, M.; Putter, H.; Muller, U. *Adv. Funct. Mater.* **2006**, *16*, 520.

(40) Sagara, T.; Klassen, J.; Ortony, J.; Ganz, E. *J. Chem. Phys.* **2005**, *123*, 014701.

(41) Hübner, O.; Gloss, A.; Fichtner, M.; Klopper, W. *J. Phys. Chem. A* **2004**, *108*, 3019.

(42) Gregg, S. J.; Sing, K. S. W. *Adsorption, Surface Area, and Porosity*; Academic Press: New York, 1967.

(43) Ruthven, D. M. *Principles of Adsorption and Adsorption Processes*; John Wiley & Sons: New York, 1984.

(44) Heuchel, M. *Langmuir* **1997**, *13*, 1150.

(45) Bojan, M. J.; Vernov, A. V.; Steele, W. A. *Langmuir* **1992**, *8*, 901.

(46) Montgomery, D. C.; Runger, G. C.; Hubele, N. F. *Engineering Statistics*, 2nd ed.; Wiley: New York, 2001.

(47) Mueller, T.; Ceder, G. *J. Phys. Chem. B* **2005**, *109*, 17974.

(48) Rosi, N. L.; Eckert, J.; Eddaoudi, M.; Vodak, D. T.; Kim, J.; O'Keeffe, M.; Yaghi, O. M. *Science* **2003**, *300*, 1127.

(49) Düren, T.; Snurr, R. Q. Proceedings of the 7th International Symposium on the Characterization of Porous Solids, Studies in Surface Science and Catalysis, in press, 2005.

(50) *Multi-Year Research, Development and Demonstration Plan*: *Planned program activities for 2003−2010*: *Technical Plan*; United States Department of Energy; http://www.eere.energy.gov/hydrogenandfuelcells/mypp/.

(51) Hinrichsen, E. L.; Feder, J.; Jossang, T. *Phys. Rev. A* **1990**, *41*, 4199.

(52) It should be noted that the random monolayer packing of 0.55 coverage corresponds to a density of hydrogen of 91 g/L and the hexagonal monolayer packing of 0.91 coverage corresponds to a density of hydrogen of 151 g/L if the height of one hydrogen molecule is used to determine the volume of the monolayer. This is the primary reason that the potential uptake values are generally higher assuming monolayer coverage than when assuming the density of liquid or solid hydrogen within the free volume.

(53) Braker, W.; Mossman, A. L. *Matheson Gas Data Book*, 6th ed.; Matheson: Secaucus, NJ, 1980.

(54) Pauling, L. *College Chemistry*: *An Introductory Textbook of General Chemistry*, 2nd ed.; W. H. Freeman & Company: San Francisco, CA, 1955.